Characterization and Imaging of Solid Lipid Nanoparticles and Nanostructured Lipid Carriers

5

Melike Üner

Contents

Keywords

Atomic force microscopy • Differential scanning calorimetry • Dynamic light scattering • Fourier transform infrared spectroscopy • Low angle laser light scattering • Nanostructured lipid carriers • Proton nuclear magnetic resonance spectroscopy • Raman spectroscopy • Scanning electron microscopy • Solid lipid nanoparticles • Transmission electron microscopy • X-ray scattering

M. Üner (✉)
Istanbul University, Faculty of Pharmacy, Department of Pharmaceutical Technology, Istanbul, Turkey
e-mail: melikeuner@yahoo.com

M. Aliofkhazraei (ed.), *Handbook of Nanoparticles*,
DOI 10.1007/978-3-319-15338-4_3

Solid lipid nanoparticles (SLN) and nanostructured lipid carriers (NLC), the second generation of SLN, are colloidal drug carrier systems that can be used for controlled drug delivery via various administration routes. They introduce various advantages over traditional dosage forms and their colloidal counterparts. SLN and NLC products are available in the market of the European community, and lipid nanotechnology has been increasingly attracted by the industry. Moreover, studies on lipid nanoparticles have been focused on targeting of drugs to the specific sites of the body, thus surface modification and treatment of SLN and NLC in the last decades. Naturally, several parameters must be taken into consideration for design of well-performing formulations, which have a long-term stability. A lot of analytical methods, which give scientists extensive informations, are essential for characterization of SLN and NLC. Investigation of factors affecting their physicochemical properties and common techniques used for their characterization will be introduced in this chapter. Determination methods of particle size, particle charge, and surface characteristics, crystallographic and structural investigations, and imaging of SLN and NLC will be discussed. In vivo and in vitro experiments will also be summarized to describe future direction of researches.

Introduction

SLN and NLC are colloidal drug carrier systems, composed of middle-chain-length triglycerides and/or waxes [1–3]. Their composition provides controlled delivery of actives. SLN and NLC are sophisticated systems suitable to administer actives including parenteral [4], oral [5], ocular [6], nasal [7], pulmonary [8], topical [9], and transdermal routes [10]. They improve tissue distribution leading to enhancement of bioavailability of entrapped actives [11]. Researchers have reported that targeting of drugs to specific organs can be possible with SLN and NLC [12–14].

SLN and NLC are safe and compatible colloidal drug carriers, which can be produced by environment-compatible techniques including high-pressure homogenization, membrane contactor method, liquid-flow focusing using microchannels or microtubes, and supercritical fluid technology. The use of organic solvents and surface active agents at high concentrations can be avoided for the production of SLN and NLC by these cost-effective techniques, which have excellent reproducibility for scaling-up [15, 16]. Various production methods else have also been reported in the literature. All techniques are listed in Table 1 with exemplary studies.

Several methods are used for characterization of SLN and NLC. Thus, informations can be obtained to reach desired formulations and to evaluate parameters affecting long-term stability of nanoparticles. These methods are based on characterization of particle size and distribution, thermal behaviors and crystallinity properties, structural properties of nanoparticles, and surface morphology (Table 2). Factors affecting parameters and common methods used for characterization of SLN and NLC will be discussed in upcoming sections.

Table 1 Exemplary studies on SLN and NLC in the literature

Method	Product/drug	Solid lipid/liquid lipid	Surfactant	References
High-pressure homogenization	SLN/tamoxifen	Softisan® 154	Phospholipon® 90 H	AL-Haj et al. [17]
	SLN and NLC/loratadine	1-Hexadecanol/Miglyol® 812	TegoCare® 450	Üner et al. (2014)
Membrane contactor method	SLN/–	Gelucire® 44/14	Tween® 20	Charcosset et al. [18]
Liquid-flow focusing using microchannels or microtubes	SLN/–	Softisan® 100	Poloxamer® 188	Yun et al. [16]
Supercritical fluid technology	SLN/caffeine	Lumulse® GMS	–	De Sousa et al. [19]
	SLN/insulin	Tristearin phosphatidylcholine	Tween® 80	Salmaso et al. [20]
Microemulsion	SLN/flurbiprofen	Beeswax and carnauba wax	Tween® 80 and egg lecithin	Baviskar et al. [21]
	NLC/celecoxib	Gelucire® 44/14/Capmul® MCM	Cremophor® RH 40	Joshi and Patravale [22]
Double emulsion (w/o/w) method	SLN/5-flurouracil (5-FU)	Dynasan® 114 Dynasan® 118	Soya lecithin and polyvinyl alcohol	Yassin et al. [23]
	SLN/yak interferon-alpha	Hydrogenated castor oil	Polyvinyl alcohol	Li et al. [24]
Solvent emulsification-evaporation	SLN/syringopicroside	Glyceryl monostearate	Pluronic® F68	Zhang et al. [25]
	SLN/efavirenz	Glyceryl monostearate	Tween® 80	Madhusudhan et al. [26]
Solvent emulsification-diffusion	SLN/etoposide	Softisan®601	Tween® 80 and Lutrol® F127	Fernandes et al. [27]
	SLN/ropinirole HLC	Stearylamine	Pluronic® F68	Pardeshi et al. [28]
High-shear homogenization	SLN/dibenzoyl peroxide	Glyceryl monostearate	Tween® 20 Tween® 80	Gardouh et al. [29]

(*continued*)

Table 1 (continued)

Method	Product/drug	Solid lipid/liquid lipid	Surfactant	References
	Erythromycin Triamcinolone acetonide			
	SLN and NLC/sildenafil citrate	Cetyl palmitate/Maisine® 35-1	Cremophor® RH 40 and Span® 85	Elnaggar et al. [30]
Ultrasonication	SLN/itraconazole	Stearic acid Palmitic acid	Polyvinyl alcohol	Mohanty et al. [31]
	NLC/–	Apifil® Compritol® 888ATO Cutina® CP Berry wax/Myritol® 312 and Cetiol®V	Plantacare® 2000UP Poloxamer® 188 TegoCare® CG-90 Crodesta® SL40LQ Tween® 80	Lasoń et al. [32]

Table 2 Characterization methods of SLN and NLC

Method	Data
Laser diffractometry	Particle size distribution
Photon correlation spectroscopy	Average particle size and particle size distribution
Zeta potential	Particle charge
Transmission electron microscopy	Particle size and imaging
Scanning electron microscopy	Particle size and imaging
Atomic force microscopy	Particle size and imaging
Differential scanning calorimetry	Thermal and crystallization behaviors of solid lipid in nanoparticles and drug-lipid interaction
X-ray diffraction	Crystallographic analysis, crystal order of lipid and drug in nanoparticles
Photon nuclear magnetic resonance spectroscopy	Nanoparticle structure and drug-lipid interaction
Fourier transform infrared spectroscopy	Nanoparticle structure and drug-lipid interaction
Raman spectroscopy	Nanoparticle structure and drug-lipid interaction

Particle Size of SLN and NLC

SLN and NLC have been explained that they are produced in the 50–1,000 nm size range with low microparticle content [33]. Particle sizes of nanoparticles are usually expected in a 50–300 nm range in the case of site-specific delivery including anticancer therapy by antineoplastic agents and genes and central nervous system disorders [34]. Then, nanoparticles must accumulate onto specific sites to provide drug delivery. Meanwhile, they are mostly required to cross several anatomic barriers. The particle size and charge with surface properties are important for site-specific delivery. For instance, nanoparticles have been proclaimed to be in an optimum size range for their accumulation in a tumor and internalization by tumor cells in the case of nanoparticles designed for targeting according to one of the strategies of site-specific delivery in cancer treatment. It is because the cutoff size of pores in tumor vessels is as large as 200 nm–1.2 mm in general. A decrease in the size of nanoparticles provides easier uptake and leads to a significant increase in the rate of cellular uptake [34]. A particle size higher than 300 nm provides sustained drug delivery in this case when the 50–300 nm size range displays rapid action.

Moreover, particle size is one of the important parameters for having information on SLN and NLC stability [35]. The particle size of lipid nanoparticles should stay in a limited size range during storage. Therefore, investigation on the change in particle size and particle size distribution in long-term stability experiments provides strict information about agglomeration and physical stability of formulations.

Various parameters affect the particle size of SLN and NLC such as composition of formulation (such as surfactant and mixture of surfactants and structural properties of the lipids and drug incorporated) and preparation process (such as choice of the preparation method, equipment, temperature, number of the cycles and pressure in the case of high-pressure homogenization, sterilization, lyophilization, and spray drying) [3, 36]. These parameters must be optimized to achieve well-formulated nanoparticles.

An increase in the concentration of surfactant(s) usually causes a decrease in particle size of lipid nanoparticles, i.e., if a higher/lipid surfactant ratio is chosen, a smaller particle size is obtained [37, 38].

The use of relatively lower-melting-point solid lipids and the increase in the oil content in the lipophilic phase of nanoparticle dispersion reduce the viscosity of the melted droplets during homogenization; thus nanoparticles form in smaller sizes.

Entrapment of drug into nanoparticles may increase the particle size [39]. Drug concentration lower than 1 % does not affect the particle size of lipid nanoparticles in general.

Processing temperature is also one of the most important parameters affecting particle size. Homogenization temperature, which is lower than the melting point of solid lipid or equal to it, results in heterogeneous particle size distribution with high microparticle content in the case of hot homogenization process. This situation is related to the viscosity of the lipophilic phase of nanoparticle dispersion during homogenization. Therefore, at least 10–15 °C higher than the melting point of a solid lipid should be preferred in hot homogenization techniques.

Homogenization efficiency increases with higher homogenization pressure. An increase in homogenization pressure up to 1,500 bar and in the number of cycles (three to seven cycles) decreases the particle size of nanoparticles [40, 41].

In general, SLN and NLC are resistant colloidal systems to lyophilization in the case of addition of proper cryoprotectant at proper concentrations. Spray drying can be used as an alternative method to lyophilization in the case of hydrolyzable drug content or a need for suitable product for per-oral administration. However, spray drying can destabilize the system due to the elevated temperature and shear forces, which increase the kinetic energy leading to frequent particle collisions [42]. Partial melting of the lipid phase during spraying is also one of the reasons for particle growth. Besides these procedures, sterilization is required for parenteral application of nanoparticles. Thus, proper sterilization (filtration, autoclaving, or gamma irradiation) technique should be chosen.

Surface modifiers to reduce phagocytic uptake of SLN and NLC for parenteral administration, such as polyethylene oxide and PEG, may increase the particle size.

Various particle size measurement techniques are used to obtain information on qualification and physical stability of SLN and NLC during storage.

Theoretically, the shape of a particle makes particle size analysis more complicated than it appears since shapes of particles vary, which makes it complicated to obtain one unique mean size [43]. One unique mean size can be obtained with perfect spherical particles which cannot be possible to obtain in practice. If the

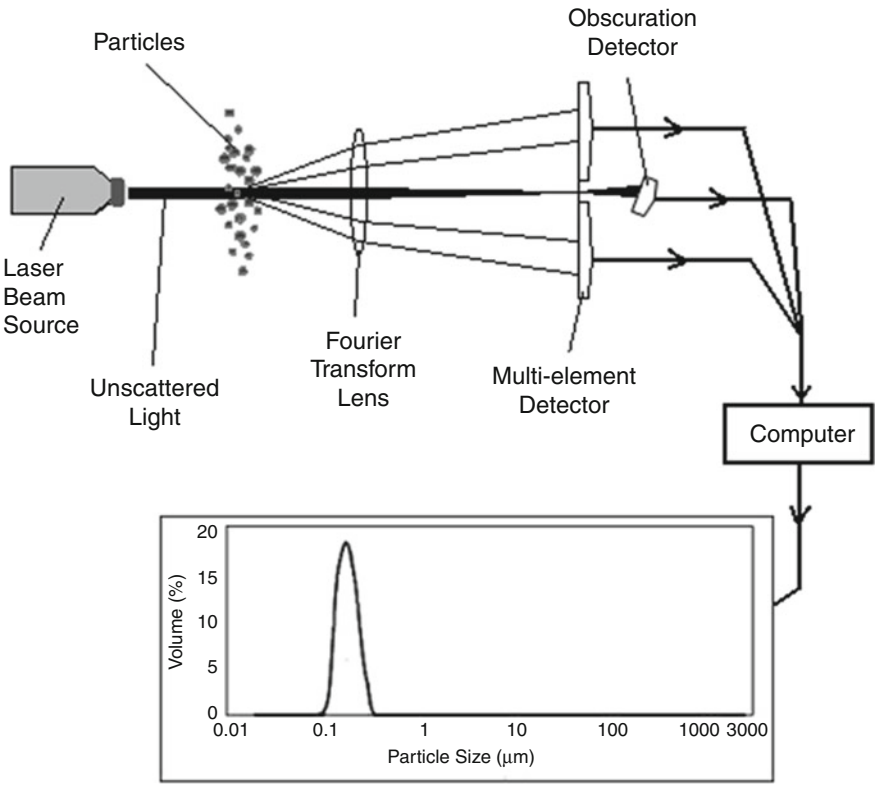

Fig. 1 Illustration and working principle of low-angle laser light scattering (*LALLS*)

shape or size of a single nanoparticle changes, its volume/weight will also change. Therefore, it will be possible to say that nanoparticles have gotten smaller/larger with an equivalent sphere model which is required for the approximation of certain values. The equivalent volume to each nanoparticle should be calculated to reach a mean number. Techniques like laser diffractometry (LD) measure proportional particle size distribution in order to provide the mean result. It should not be forgotten that different techniques give different means.

LD and photon correlation spectroscopy (PCS) are commonly used for characterizing particle size of lipid nanoparticles and their particle size distribution.

Laser Diffractometry (LD)

This technique, which is used for obtaining information on particle size distribution and microparticle content of SLN and NLC, is also called low-angle laser light scattering (LALLS) [44]. In a laser diffractometer, a laser beam passes through the sample in a laser scattering cell (Fig. 1). The laser is scattered with a diffraction

angle inversely proportional to particle size when it interacts to the nanoparticles. The intensity of scattering is detected by a suitable detector. Then, data gives information on the volume distribution of the sample.

LALLS is used for the characterization of particles for the range of 0.05–3,500 μm typically. He-Ne gas lasers ($\lambda = 0.63$ μm) are one of the most commonly used lasers since they display the best stability, especially in respect to temperature. They give better and more reliable signals to noise than the higher-wavelength laser diodes.

Using the Mie theory introduces advantages over the Fraunhofer approximation since it provides the volume of the particle as opposed to the Fraunhofer approximation, which gives a projected area prediction. It is also capable to solve the equations for the interaction of light with matter through LALLS instruments. Nanoparticle dispersions and powders can be measured directly with LALLS within 1 min. 4–10 g and 1–2 g samples are required for dry powders and dispersions in the measurements, respectively. LALLS is a nondestructive and nonintrusive method. Therefore, samples can be recovered if it is required.

Photon Correlation Spectroscopy (PCS)

PCS is also called dynamic light scattering (DLS) and quasi-elastic light scattering (QELS). DLS is used to measure particle size in submicron range using their Brownian motion in aqueous media [44]. In this technique, a laser beam is sent through the nanoparticle dispersion and scattering light is detected by a photomultiplier, which is positioned at a scattering angle of 90° (Fig. 2). Therefore, nonlinearity of the light can be avoided with the scattering angle. The scattered light causes a signal, which is received by a photomultiplier. The photomultiplier transforms intensity variations into a variation of voltage evaluating the signal with a correlation function. It is because small particles diffuse faster and lead to more rapid fluctuation of the intensity of the light scattered compared to larger particles.

DLS measurements also provide polydispersity index (PI), the width of particle size distribution of samples in the area of light scattering [45]. PI is calculated via an intensity autocorrelation function using a cumulant analysis of DLS.

Several advantages of DLS have been reported in the literature [44, 46]. One of them is that a minimum number of particles are needed, i.e., around 100 particles are sufficient for the measurements. The measurement results can be obtained within 1 min. DLS is also a nondestructive and nonintrusive method. Therefore, samples can be recovered if it is required. Although DLS is the most powerful technique for particle size measurements of SLN and NLC, it has various limitations like problems that occurred in the cases of a sample with broad particle size distribution, multimodal distribution, and nonspherical particles. Additionally, it must be paid attention to measurement conditions and related details such as temperature, refractive index, and/or viscosity.

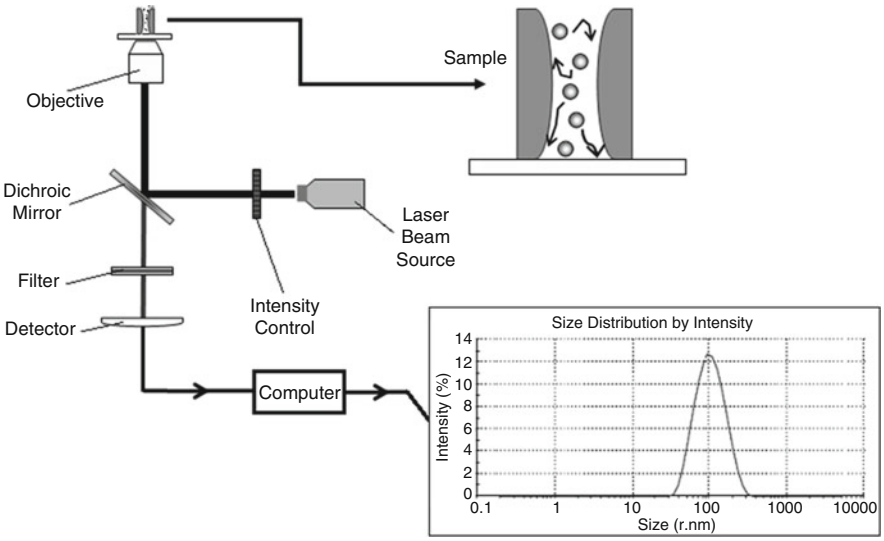

Fig. 2 Illustration of dynamic light scattering (*DLS*) and its working principle

Particle Charge (Zeta Potential) of SLN and NLC

The nature of the electrostatic potential near the surface of a particle is called the zeta potential (ZP). The amount of charge on the particle surface is one of the important characteristics giving information on the tendency of nanoparticles to agglomerate and on their long-term stability [3, 40]. SLN and NLC may have a surface charge, which attracts a thin layer of ions of opposite charge to the nanoparticle surface. This double layer of ions travels with the nanoparticle as it diffuses throughout the solution [47]. ZP is the electric potential at the boundary of the double layer. ZP has values that typically range from +100 to −100 mV. There are several reasons for increasing ZP of lipid nanoparticles. The surface of nanoparticles containing chemical groups may ionize to produce a charged surface. Or ZP increases with ionic surfactant. If ionic lipids or drugs are used for the preparation of SLN and NLC, nanoparticles give higher ZP values. Sometimes the surface itself preferentially adsorbs ions.

In general, a ZP greater than −60 mV is known to require for excellent physical stability of nanoparticles when greater than −30 mV indicates good electrostatic stabilization and good physical stability [48]. Nevertheless, this rule cannot be applied strictly for every colloidal drug carrier system which contains steric stabilizers because the adsorption of nonionic steric stabilizers usually decreases ZP due to the shift in the shear plane of the particle [49].

An increase in the kinetic energy caused by light and temperature decreases ZP and leads to frequent particle collisions.

Changes in the crystalline structure of lipid in nanoparticles may also lead to a change in the particle charge [48]. In a coherent manner, the ZP of dispersions may decrease after autoclaving, particularly for nanoparticles composed of fatty acids [50].

ZP is an important parameter for systemic half-life and biodistribution of nanoparticles when it is critical for the long-term stability of SLN and NLC. Besides the nature of lipids and surface actives used for the preparation of SLN and NLC, coating materials contribute to the surface charge of nanoparticles [51, 52]. Negatively charged nanoparticles usually have longer systemic half-life compared to positively charged nanoparticles when strongly negative and strongly positive charges usually lead to phagocytic uptake of nanoparticles more rapidly than weak-medium negative charge.

ZP is determined by measuring the velocity of the particles in an electric field. For this purpose, a DLS apparatus or a zetasizer may be used. The laser beam, which is sent to pass through the center of the sample cell is scattered at an angle of 17°. Scattered light is detected and the type of ZP of the sample is recognized by the system configuration.

Imaging of SLN and NLC

Particle size measurements and imaging of nanoparticles can be made by electron microscopy [53]. Structural details of SLN and NLC can be visualized with this technique since the spatial resolution can be usually achieved at around 0.2 nm. Electrons are used instead of light for the imaging of objects in electron microscopy [54]. The resolving power of an electron microscope is a linear function of the wavelength. Therefore, electrons with wavelengths about 100,000 times shorter than the photons of visible light provide for a resolution better than 50 pm [55]. Electrons, which are sent through the sample, interact with the constituent atoms via electrostatic forces (Coulomb forces) in an electron microscope. Thus, some electrons are scattered. Electrons are focused, collected, and processed to acquire a two-dimensional projected image of the three-dimensional sample structure.

Atomic force microscopy (AFM), which is based on scanning sample surface, is also commonly used for the imaging of SLN and NLC.

Transmission Electron Microscopy (TEM)

A transmission electron microscope contains an illumination system, which takes the electron from a gun and transfers them to the sample (Fig. 3). Then, the sample can be screened by a computer using several consecutive lenses. A TEM imaging system contains objective, condenser, intermediate, and projector lenses. If the system is adjusted to the diffraction mode, the back focus plane is taken as the objective plane of the intermediate and projector lenses. Thus, the diffraction pattern is obtained on the screen. Alternatively, if the system is adjusted to the

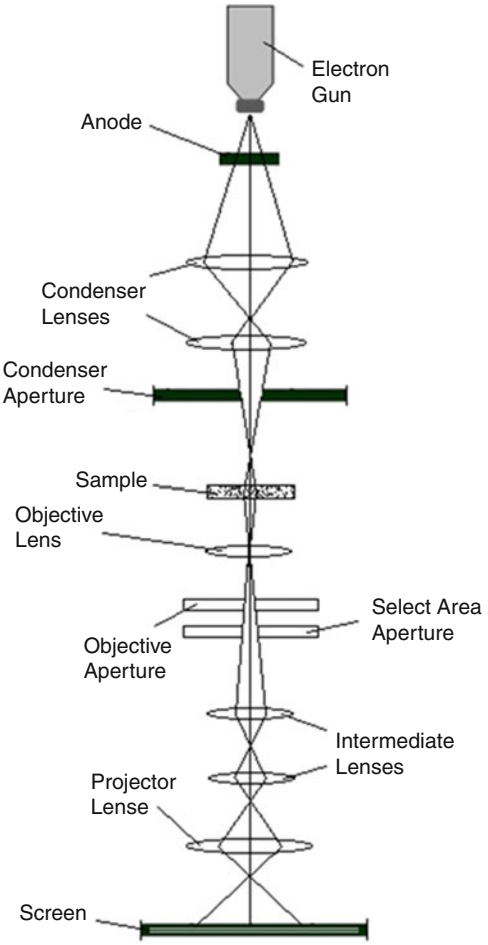

Fig. 3 Illustration and working principle of transmission electron microscopy (*TEM*)

image mode, the image plane of the objective lens is used as the objective plane of the intermediate and projector lenses. Then, the image forms on the screen. The second system mode is more commonly used for imaging and surface characterization of SLN and NLC [56]. Images of lipid nanoparticles obtained by TEM are seen in Fig. 4 as an example [57].

Scanning Electron Microscopy (SEM)

A focused electron beam scans across the surface of a solid sample point by point to acquire the image in SEM [54]. Electrons, which are sent through the sample, are

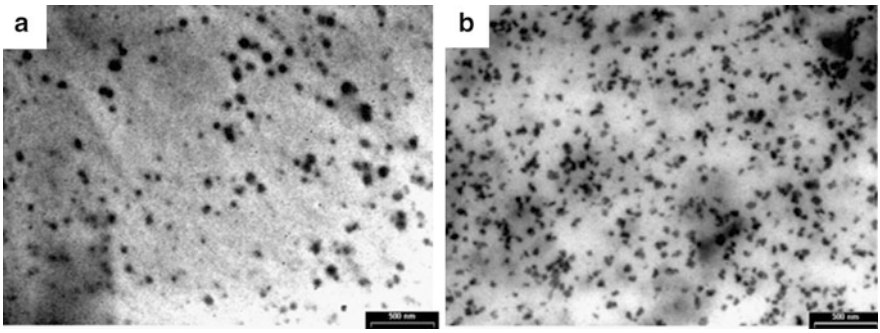

Fig. 4 TEM images of molecular sunscreen nanoparticles based on *n*-hexadecyl palmitate and glyceryl stearate (Reproduced from Lacatusu et al. [57] with the Permission of Springer)

deflected by a large number of elastic scattering processes (Fig. 5). The energy spectrum emerged by the deflection of electrons is collected by the detector. The system configures the data in different types of contrast. Large areas of samples can be investigated with a high depth of focus. The depth of focus allows a special image formation since projecting areas cast shadows when recessed areas appear dark. Therefore, the image enables the human eye to interpret and readily comprehend the obtained information (Fig. 6) [58].

Atomic Force Microscopy (AFM)

Atomic force microscopy (AFM), which is a three-dimensional topographic technique with a high atomic resolution, is based on scanning a sample surface with a probe and on imaging surface properties of the sample [59]. An atomic force microscope is operated to measure force between the probe and the sample (Fig. 7). A tip is attached to the probe of a cantilever. AFM tips and cantilevers are microfabricated from Si or Si_3N_4. The tip is designed typically as a pyramidal sharp tip.

AFM relies on the forces between the tip and sample. Thus, these forces must be correctly measured to provide a proper imaging of the sample. The force is not measured directly; it must be calculated by measuring the deflection of the lever considering the stiffness of the cantilever. The optical lever operates by reflecting a laser beam off the cantilever. A four-segment photodetector, which is position sensitive, detects the reflected laser beam striking. The differences between the signals produced by the segments of the photodetector of signals display the position of the laser spot on the detector and the angular deflections of the cantilever. An atomic force microscope can generally measure the vertical and lateral deflections of the cantilever by using the optical lever for obtaining the image resolution. In general, lateral and vertical resolution of AFM can be up to 30 and 0.1 nm, respectively.

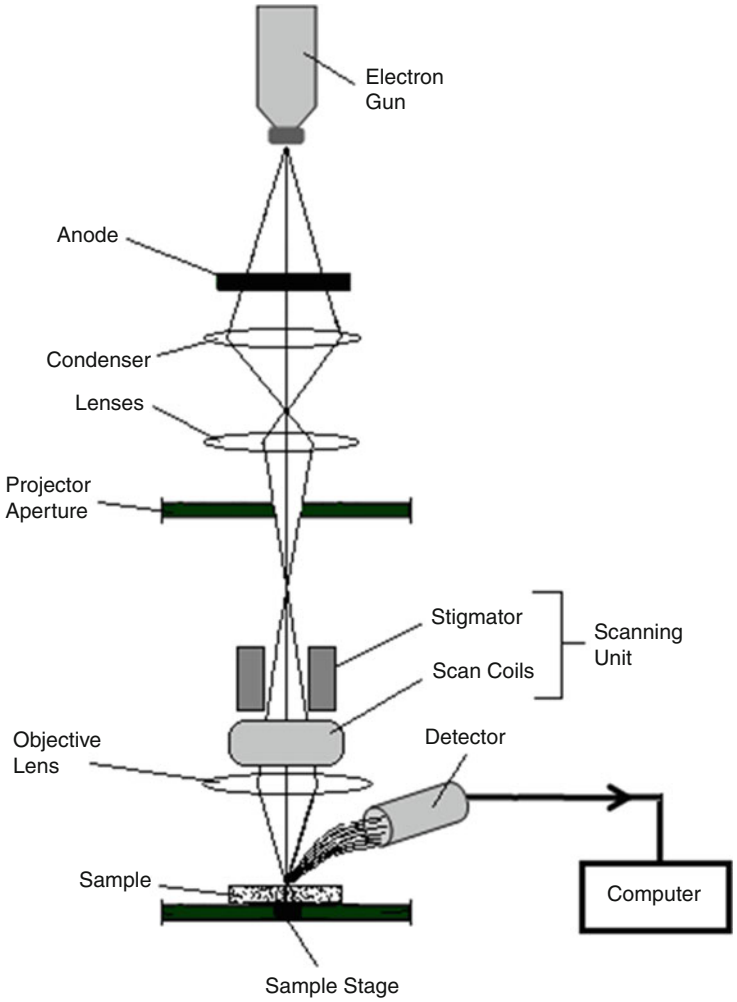

Fig. 5 Illustration and working principle of scanning electron microscopy (*SEM*)

AFM is a versatile technique for imaging since it can be applied to samples in a wide range of characteristics and a microscope can be modified (lateral force microscopy and force modulation) or operated in different modes (dynamic force tapping, contact, noncontact, and phase modes) suitable for different samples. Tapping, contact, and noncontact modes are commonly used for the imaging of SLN and NLC [60–63].

In the case of the contact mode of the microscope, the system uses feedback to regulate the force on the sample. It measures the force on the sample regulating it, thus allowing acquisition of images at very low forces. The feedback loop controls the height of the tip attached to the cantilever and optical lever. Microscope performance depends on appropriate construction and operation of the feedback loop.

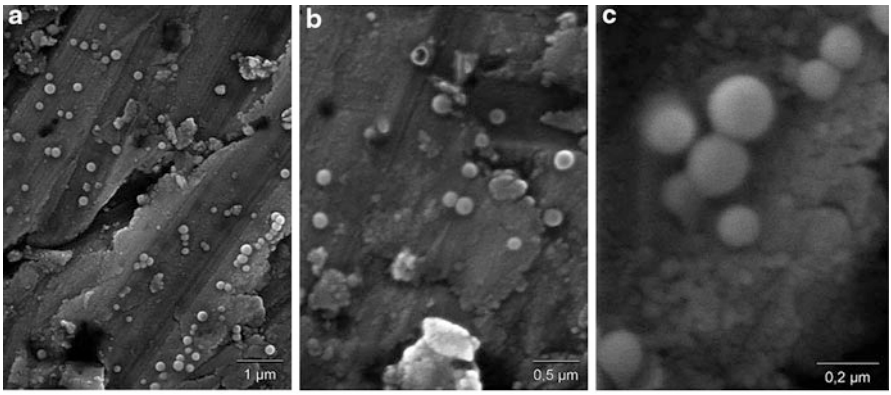

Fig. 6 SEM images of SLN derived from 2,3-di-*o*-alkanoyl-b-cyclodextrin, scale bar: (**a**) 1 µm, (**b**) 0.5 µm, and (**c**) 0.2 µm (Reproduced from Dubes et al. [58] with the Permission of Elsevier)

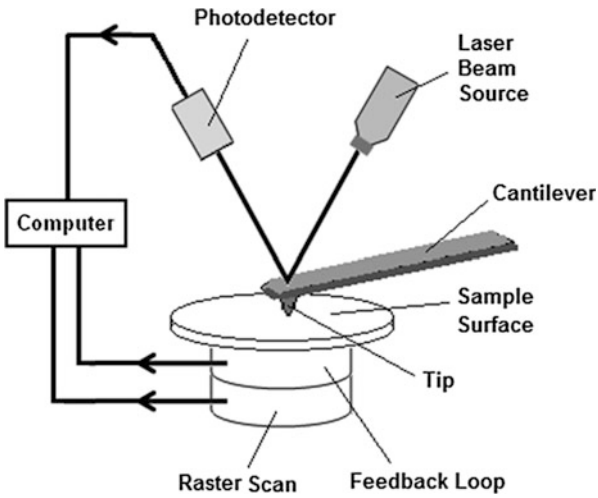

Fig. 7 Illustration and working principle of atomic force microscopy (*AFM*)

Dynamic force mode (intermittent contact) is commonly referred as the tapping mode. It is an advantageous method since an improved lateral resolution on soft samples can be obtained. This technique is preferable for poorly adsorbed samples on a substrate surface. In this mode, very stiff cantilevers are required and the cantilever is oscillated close to the sample but not touching it. A repulsive regime is applied to the oscillation, and then the tip is allowed to intermittently touch or tap the sample surface (Fig. 8) [60].

In the noncontact mode, a stiff cantilever is adjusted to a close position to the sample without touching it and is given oscillation in the attractive regime. The detection is based on measuring changes to the resonant frequency or amplitude of the cantilever (Fig. 9) [63].

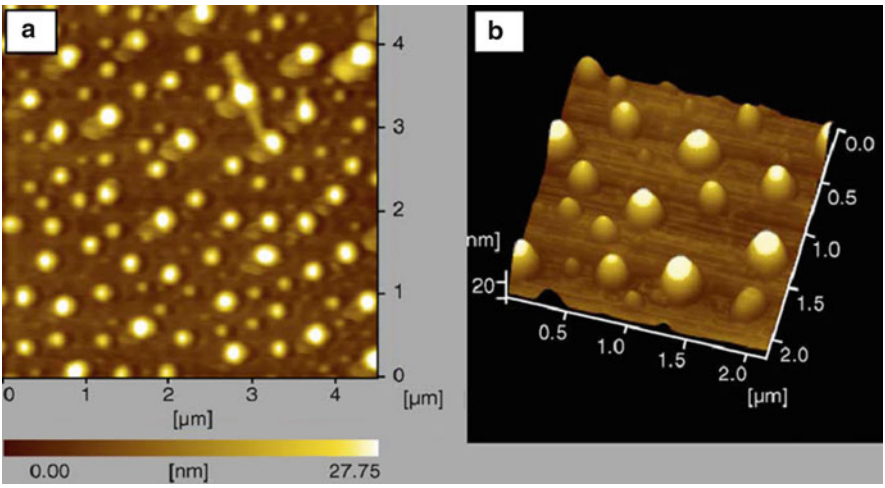

Fig. 8 Tapping mode AFM image of podophyllotoxin-loaded SLN (Reproduced from Chen et al. [60] with the Permission of Elsevier)

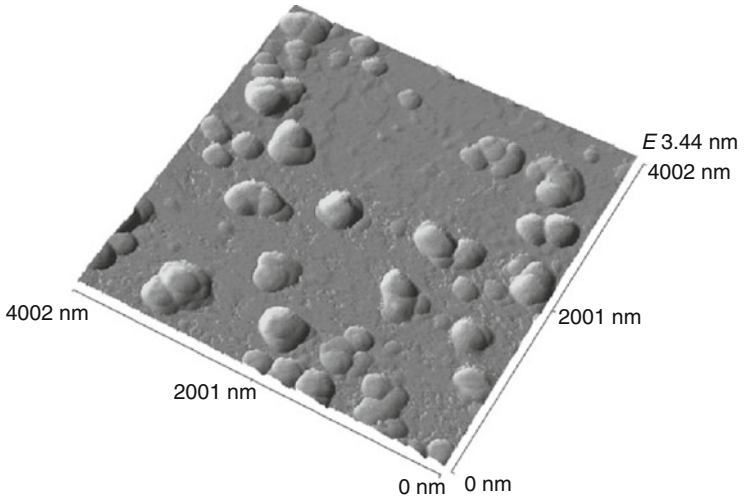

Fig. 9 Noncontact mode AFM image of *para*-acyl-calix-arene-based SLN (Reproduced from Shahgaldian et al. [63] with the Permission of Elsevier)

Crystal Properties of SLN and NLC (Crystallographic Analysis)

The crystallization and solidification properties of solid lipids are fundamental behaviors to understanding and optimizing SLN and NLC dispersions to obtain stable formulations. Subsequently, polymorphic transition, crystallization

temperature, and crystallization degree of the solid lipid in nanoparticles must be paid special attention. Hot nanoemulsion obtained using a solid lipid in the lipophilic phase of the dispersion must be cooled down below the critical crystallization temperature of the lipid to crystallize and to acquire nanoparticles after the homogenization process. If the critical temperature is not reached, particles remain in the liquid state. Hence, a supercooled emulsion is obtained instead of the desired product containing lipid nanoparticles in the solid state.

The polymorphic transition to a more stable lipid polymorph is attended by the rearrangement of the lipid molecules with an increase in lattice density [3, 40, 64]. The melting process requires lower energy in amorphous crystal or a less ordered state of the lipid compared to the perfect crystalline substance to overcome lattice forces. Therefore, a higher-ordered lattice arrangement gives a higher melting enthalpy. Although the lipid nanoparticles are produced from solid bulk lipids in the crystalline state, the lipid in SLN and NLC occurs in a less ordered arrangement [65, 66]. The crystallization behavior (degree of crystallinity and formation of crystal modifications) of a solid lipid in nanoparticles is affected by some factors including production method, concentration of solid lipid and surfactant(s), melting point of the lipid, incorporation of a liquid lipid, drug incorporation, and particle size of the resulting system [67]:

- The polymorphic transition process of the lipid in nanoparticles is defined by the type of homogenization. Lipid is provided in the solid state in the cold homogenization technique that the lipid melt is solidified in liquid nitrogen and homogenization is performed at room temperature or below. However, recrystallization of solid lipid delays in the hot homogenization technique [36].
- Lipid concentration lower than 5 % w/w disturbs the formation of crystals when crystallization is delayed with an increase in surfactant concentration [68].
- There is a converse relationship between the melting point of the lipid and the rate of the polymorphic transition.
- The type of surfactant(s) is critical for the kinetics of polymorphic transition of lipids and the crystallization temperature of the dispersed phase. The stabilizers not only influence the colloidal state of the dispersion (e.g., with respect to particle size and stability) but may also have pronounced effects on the internal structure of the particles, which is also an important parameter for the development of drug carriers based on lipid nanosuspensions [37].
- Incorporation of a liquid lipid into the solid lipid matrix of nanoparticles disturbs crystal formation and creates amorphous regions in the structure. Hence, recrystallization behavior and transformation to the more stable forms of the solid lipid are delayed during storage.
- Incorporation of drug usually prevents the formation of unstable modifications and accelerates the transformation to the stable polymorph [35, 69].
- Crystalline structures are distorted by the high surface-to-volume ratio of lipid nanoparticles. This distortion induces depression of the melting point and recrystallization point of lipid nanoparticles. A small particle size may cause formation of liquid, amorphous, or only partially crystallized metastable systems [70].

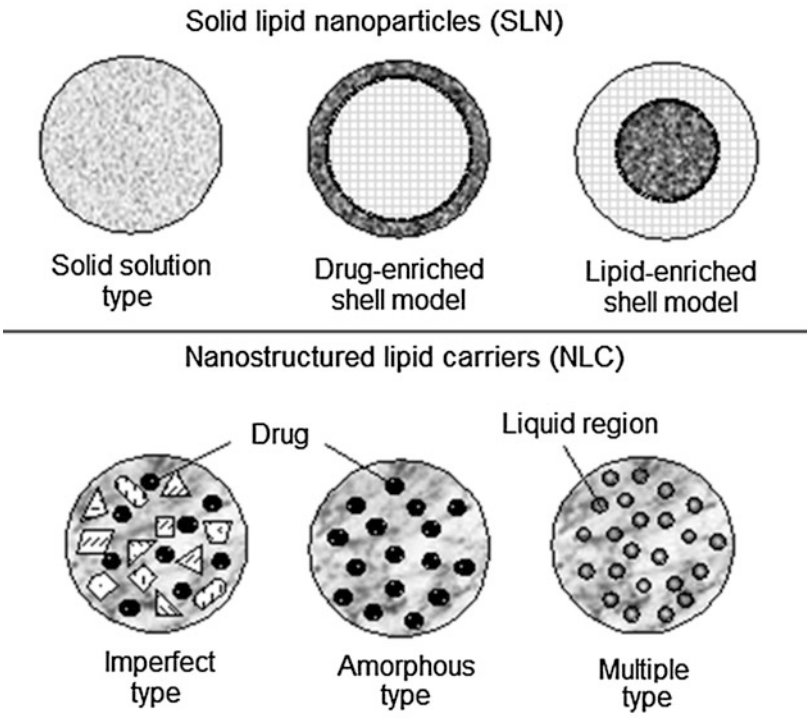

Fig. 10 Types of SLN and NLC

Polymorphic transition to the stable form of the lipid may lead to drug expulsion from nanoparticles during storage [37]. Additionally, drug payload and drug release rate are relevant to crystallinity characteristics of the lipid [71]. A less ordered arrangement of the lipid crystals increases the drug-loading capacity [64].

The incorporation of a liquid into nanoparticles provides several benefits in order to overcome some limitations occurred along with SLN [51]. Drug loss during storage may be possible due to the lipid crystallization in SLN to the stable β-modification. However, NLCs, which have special structures, provide an increase in drug payload and prevent drug expulsion with better drug accommodation. The liquid lipid inside nanoparticles provides different types of NLC with large distances between fatty acid chains (imperfect type), structureless solid amorphous matrix (amorphous type), or liquid regions (oily nanocompartments) (multiple type) (Fig. 10).

Differential scanning calorimetry (DSC), X-ray diffraction, and high-resolution proton nuclear magnetic resonance (H^1 NMR) spectroscopy are commonly used to investigate thermodynamic behaviors and state of lipid in SLN and NLC. Additionally, structural analyses like Fourier transform infrared (FT-IR) spectroscopy and Raman spectroscopy may also help to understand supramolecular characteristics.

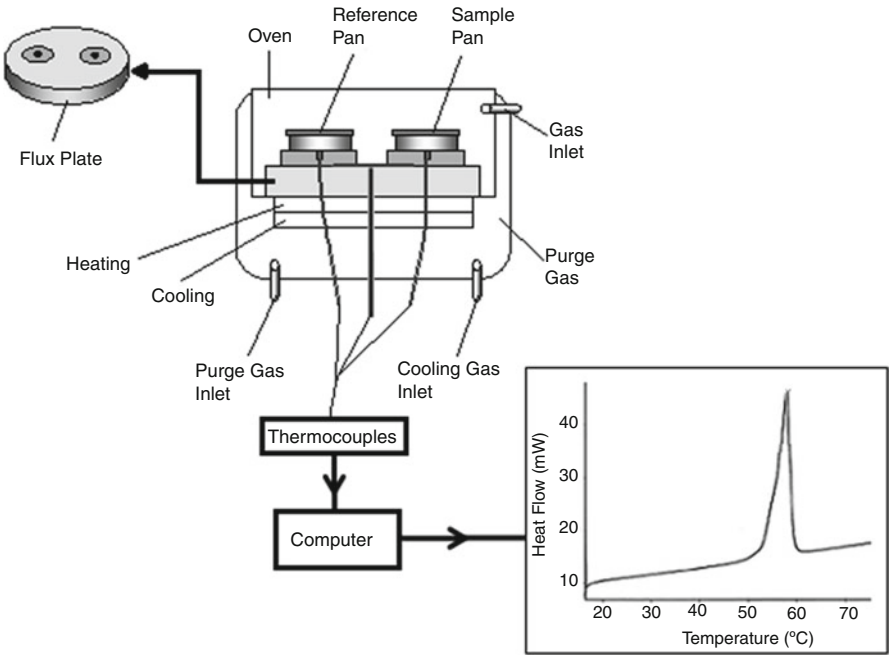

Fig. 11 Illustration and working principle of differential scanning calorimetry (*DSC*)

Differential Scanning Calorimetry (DSC)

DSC experiments are used for investigation of the melting and crystallization behavior of lipid nanoparticles. Internal polymorphism and crystal ordering of solid lipid and breakdown or fusion of crystal lattice can be defined by heating or cooling a sample [72]. DSC is also useful to obtain information about simple eutectic mixtures, solid dispersions like solid solutions, drug-lipid interactions, and the mixture behavior of solid and liquid lipids [3, 40]. DSC experiments are based on the fact that different lipid modifications possess different melting points and enthalpies [15].

The principle of DSC is based on the measurement of the difference in the amount of heat required to increase the temperature of a sample and reference (typically an empty pan) as a function of temperature (Fig. 11). When the sample undergoes a polymorphic transition, more or less heat will need to flow to it than to the reference to maintain both at the same temperature. When solid lipid melts, it requires more heat flowing to increase its temperature at the same rate as the reference. The lipid absorbs heat and undergoes the endothermic phase transition from solid to liquid. More or less heat flow to the sample depends on whether the process is exothermic or endothermic. As the sample undergoes exothermic processes such as crystallization, less heat is required to raise the sample temperature. Therefore, the difference in heat flow between the sample and reference can be measured observing the amount of heat absorbed or released during

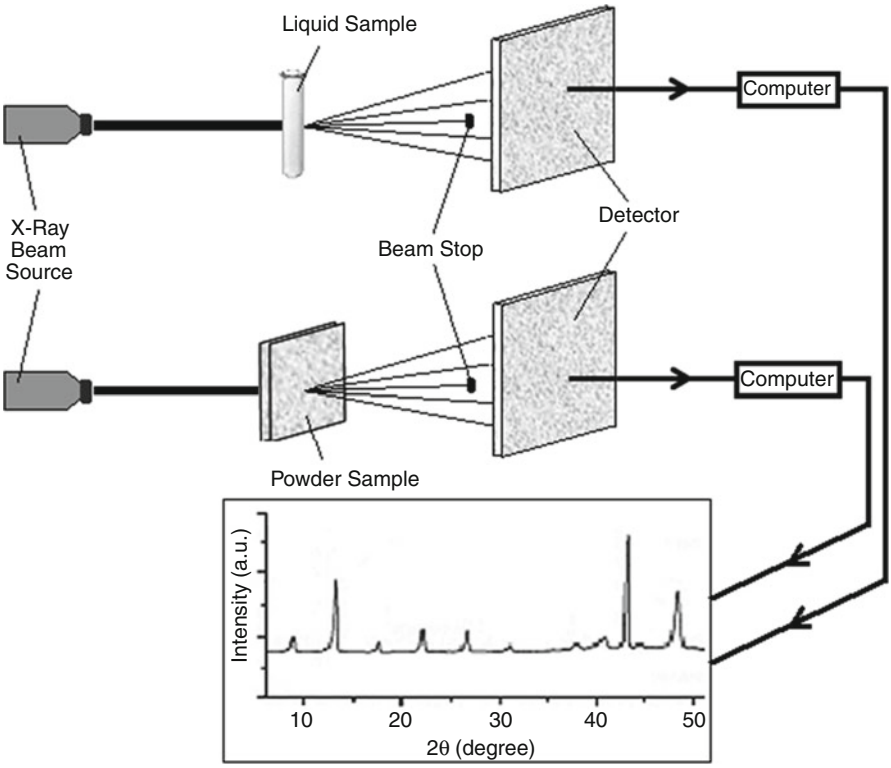

Fig. 12 Illustration and working principle of wide-angle X-ray scattering (*WAXS*) and small-angle X-ray scattering (*SAXS*)

such transitions. DSC can also be used for determination of more subtle phase changes like glass transitions.

X-Ray Diffraction

A solid lipid in SLN and NLC exhibits different crystalline species during storage. The polymorphism of the solid lipid is observed because alkane chains are locally organized in α, β′, and β packing [73–75]. The hexagonal α packing is the most disordered, the orthorhombic β′ is less disordered, and the well-organized β exhibits a triclinic packing. When thermodynamic stability increases with crystal order, it is decreased by crystallization kinetics. Lipid chains exhibit tilts and molecular conformation in the layers. X-ray diffraction experiments provide information on the length of the long and short spacings of the lipid lattice (Fig. 12). Packings in the range of 3–5 Å can be characterized by wide-angle X-ray scattering (WAXS) [76, 77]. However, layer thickness in the range of 20–50 Å can be characterized by small-angle X-ray scattering (SAXS) [78, 79].

Structural Analysis of SLN and NLC

Proton Nuclear Magnetic Resonance (H^1-NMR) Spectroscopy

H^1-NMR spectroscopy is based on the fact that the energy required to cause a nuclear spin flip is a function of the magnetic environment experienced by the nucleus [80]. An atomic nucleus possesses a nuclear spin and thus a permanent magnetic dipole moment. A charged particle like a nucleus or an electron in motion generates a magnetic field. In the case of an external magnetic field, the magnetic moment (spin) of 1H nucleus, which represents a proton in resonance, becomes aligned with the external field of lower energy or against it at the higher energy. The number, position, relative intensity, and splitting of signals are detected in H^1-NMR spectroscopy in order to obtain information on the molecular structure of the sample.

H^1-NMR spectroscopy is commonly used for the characterization of lipid nanoparticles, presenting the statement of the liquid lipid contained in SLN (i.e., NLC) and the drug [81, 82]. The arrangement and mobility of molecules of the liquid lipid can be defined by H^1-NMR measurements. Moreover, H^1-NMR spectroscopy is also suitable to deduce drug distribution and to obtain information on the mobility of the drug molecules within nanoparticles [82, 83].

Fourier Transform Infrared Spectroscopy (FT-IR) and Raman Spectroscopy

Fourier transform infrared (FT-IR) spectroscopy is developed to overcome some limitations related to traditional IR. Thus, a number of advantages have been provided such as increased sensitivity and improved data processing and scanning speed. In this method, a broadband of different wavelengths of infrared radiation is emitted by an IR source and it is sent through an interferometer that modulates the infrared radiation. The modulated IR beam passes through the sample and it is absorbed to various extents at different wavelengths by the various molecules present. The intensity of the IR beam passed is detected by a detector, and data is configurated by the system software to obtain an FT-IR graph.

Raman spectroscopy is a vibrational spectroscopy technique. Its working principle is based on the emission and absorption of infrared and visible light. This technique differs than IR since it can detect changes that do not involve dipole moment. Raman spectroscopy requires a change in dipole moment and polarizability of a molecule according to its vibration.

Both of the methods are employed to obtain conformational information about lipid molecules (solid and liquid lipids or their mixture) in a dispersion [84, 85]. Thus, information on physicochemical changes, drug-excipient interaction, and chemical compatibility of ingredients in SLN and NLC dispersions can be obtained during storage [26, 29].

Conclusion

Besides physicochemical experiments, SLN and NLC may also be evaluated considering their drug release characteristics, biodistribution properties, and movement capability through tissues by researchers.

The drug release characteristics of SLN and NLC are important parameters, which are required to investigate by in vitro experiments and to evaluate by considering mathematical models. They are strongly affected by the drug incorporation model, crystallization behaviors, and particle size of nanoparticles. The capability of nanoparticles for controlled drug delivery may define pharmaceutical quality of SLN and NLC dispersion. For an instance, drug release with burst effect within 10 min is an undesirable situation for parenteral application of SLN and NLC. A well-formulated system should protect most of its drug content until it reaches the targeted organ or tissues in the case of site-specific delivery. The site-specific delivery of nanoparticles is investigated by cell culture, ex vivo, and in vivo experiments.

For site-specific delivery of nanoparticles, their several biological properties must be known. Information on efficiency of surface treatment of nanoparticles; their stability in the systemic circulation, phagocytosis, opsonization, and endocytosis; and then their activity in tissues/cells can be acquired by cell culture experiments. The cytotoxicity of nanoparticles loaded with antineoplastics is also observed. In the case of well-formulated nanoparticles, drugs or genes can be delivered with maximal efficacy and potency and minimal side effects.

Ex vivo studies with organic materials obtained from human and experiment animals and in vivo studies give the most reliable and definite results.

SLN and NLC are sophisticated colloidal drug carrier systems, which have unique properties and a lot of advantages over traditional dosage forms and their colloidal counterparts. They are promising for the treatment of genetical disorders and deadly illnesses like cancer. Various research groups and pharmaceutical companies are increasingly attracted with SLN and NLC. Successful results obtained from physicochemical experiments and in vivo, ex vivo, and in vitro studies indicate SLN and NLC as promising colloidal drug carrier systems for the selective delivery of actives in the near future.

References

1. R. Abbasalipourkabir, A. Salehzadeh, R. Abdullah, Characterization and stability of nanostructured lipid carriers as drug delivery system. Pak. J. Biol. Sci. **15**, 141–146 (2012)
2. M.A. Iqbal, S. Md, J.K. Sahni et al., Nanostructured lipid carriers system: recent advances in drug delivery. J. Drug Target. **20**, 813–830 (2012)
3. W. Mehnert, K. Mäder, Solid lipid nanoparticles: production, characterization and applications. Adv. Drug Deliv. Rev. **64**, 83–101 (2012)
4. K.K. Sawant, S.S. Dodiya, Recent advances and patents on solid lipid nanoparticles. Recent Pat. Drug Deliv. Formul. **2**, 120–135 (2008)
5. B.D. Patel, R.V. Modi, N.A. Thakkar et al., Development and characterization of solid lipid nanoparticles for enhancement of oral bioavailability of raloxifene. J. Pharm. Bioallied Sci. **4** (Suppl 1), S14–S16 (2012)

6. K. Hippalgaonkar, G.R. Adelli, K. Hippalgaonkar et al., Indomethacin-loaded solid lipid nanoparticles for ocular delivery: development, characterization, and in vitro evaluation. J. Ocul. Pharmacol. Ther. **29**, 216–228 (2013)
7. A.S. Joshi, H.S. Patel, V.S. Belgamwar et al., Solid lipid nanoparticles of ondansetron HCl for intranasal delivery: development, optimization and evaluation. J. Mater. Sci. Mater. Med. **23**, 2163–2175 (2012)
8. W. Wang, R. Zhu, Q. Xie et al., Enhanced bioavailability and efficiency of curcumin for the treatment of asthma by its formulation in solid lipid nanoparticles. Int. J. Nanomed. **7**, 3667–3677 (2012)
9. G. Niculae, I. Lacatusu, N. Badea et al., Lipid nanoparticles based on butylmethoxydibenzoylmethane: in vitro UVA blocking effect. Nanotechnology **23**, 315704 (2012)
10. G. Shiva, M. Somaye, J.M. Reza, Improved photostability, reduced skin permeation and irritation of isotretinoin by solid lipid nanoparticles. Acta Pharm. **62**, 547–562 (2012)
11. T. Jie, X. Pang, Y. Kefu et al., Preparation, characterization and in vivo distribution of solid lipid nanoparticles loaded with cisplatin. Pharmazie **8**, 593–597 (2008)
12. N. Chattopadhyay, J. Zastre, H.L. Wong et al., Solid lipid nanoparticles enhance the delivery of the HIV protease inhibitor, atazanavir, by a human brain endothelial cell line. Pharm. Res. **25**, 2262–2271 (2008)
13. L. Reddy, R. Sharma, K. Chuttani et al., Etoposide-incorporated tripalmitin nanoparticles with different surface charge: formulation, characterization, radiolabeling, and biodistribution studies. AAPS J. **6**, 55–64 (2004)
14. Y.H. Yu, E. Kim, D.E. Park et al., Cationic solid lipid nanoparticles for co-delivery of paclitaxel and siRNA. Eur. J. Pharm. Biopharm. **80**, 268–273 (2012)
15. R.H. Müller, K. Mäder, S. Gohla, Solid lipid nanoparticles (SLN) for controlled drug delivery-a review of the state of the art. Eur. J. Pharm. Biopharm. **50**, 161–177 (2000)
16. J. Yun, S. Zhang, S. Shen et al., Continuous production of solid lipid nanoparticles by liquid flow-focusing and gas displacing method in microchannels. Chem. Eng. Sci. **64**, 4115–4122 (2009)
17. N.A. Al-Haj, R. Abdullah, S. Ibrahim et al., Tamoxifen drug loading solid lipid nanoparticles prepared by hot high pressure homogenization techniques. Am. J. Pharmacol. Toxicol. **3**, 219–224 (2008)
18. C. Charcosset, A. El-Harati, H. Fessi, Preparation of solid lipid nanoparticles using a membrane contactor. J. Control. Release **108**, 112–120 (2005)
19. A.R.S. De Sousa, A.L. Simplício, H.C. De Sousa et al., Preparation of glyceryl monostearate-based particles by PGSS®-Application to caffeine. J. Supercrit. Fluids **43**, 120–125 (2007)
20. S. Salmaso, N. Elvassore, A. Bertucco et al., Production of solid lipid submicron particles for protein delivery using a novel supercritical gas-assisted melting atomization process. J. Pharm. Sci. **98**, 640–650 (2009)
21. D.T. Baviskar, A.S. Amritkar, H.S. Chaudhari et al., Modulation of drug release from nanocarriers loaded with a poorly water soluble drug (flurbiprofen) comprising natural waxes. Pharmazie **67**, 701–705 (2012)
22. M. Joshi, V. Patravale, Nanostructured lipid carrier (NLC) based gel of celecoxib. Int. J. Pharm. **346**, 124–132 (2008)
23. A.E. Yassin, M.K. Anwer, H.A. Mowafy et al., Optimization of 5-flurouracil solid-lipid nanoparticles: a preliminary study to treat colon cancer. Int. J. Med. Sci. **7**, 398–408 (2010)
24. S. Li, B. Zhao, F. Wang et al., Yak interferon-alpha loaded solid lipid nanoparticles for controlled release. Res. Vet. Sci. **88**, 148–153 (2010)
25. X. Zhang, S. Lü, J. Han et al., Preparation, characterization and in vivo distribution of solid lipid nanoparticles loaded with syringopicroside. Pharmazie **66**, 404–407 (2011)
26. A. Madhusudhan, G.B. Reddy, M. Venkatesham et al., Design and evaluation of efavirenz loaded solid lipid nanoparticles to improve the oral bioavailability. Int. J. Pharm. Pharm. Sci. Res. **2**, 84–89 (2012)
27. C.B. Fernandes, S. Mandawgade, V.B. Patravale, Solid lipid nanoparticles of etoposide using solvent emulsification diffusion technique for parenteral administration. Int. J. Pharm. Biosci. Technol. **1**, 27–33 (2013)

28. C.V. Pardeshi, P.V. Rajput, V.S. Belgamwar et al., Novel surface modified solid lipid nanoparticles as intranasal carriers for ropinirole hydrochloride: application of factorial design approach. Drug Deliv. **20**, 47–56 (2013)
29. A.R. Gardouh, S. Gad, H.M. Ghonaim et al., Design and characterization of glyceryl monostearate solid lipid nanoparticles prepared by high shear homogenization. Br. J. Pharm. Res. **3**, 326–346 (2013)
30. Y.S.R. Elnaggar, M.A. El-Massik, O.Y. Abdallah, Fabrication, appraisal, and transdermal permeation of sildenafil citrate-loaded nanostructured lipid carriers versus solid lipid nanoparticles. Int. J. Nanomed. **6**, 3195–3205 (2011)
31. B. Mohanty, D.K. Majumdar, S.K. Mishra et al., Development and characterization of itraconazole-loaded solid lipid nanoparticles for ocular delivery. Pharm. Dev. Technol **20**, 458–464 (2015)
32. E. Lasoń, E. Sikora, J. Ogonowski, Influence of process parameters on properties of nanostructured lipid carriers (NLC) formulation. Acta Biochim. Pol. **60**, 773–777 (2013)
33. S.S. Shidhaye, R. Vaidya, S. Sutar et al., Solid lipid nanoparticles and nanostructured lipid carriers-innovative generations of solid lipid carriers. Curr. Drug Deliv. **5**, 324–331 (2008)
34. F. Wan, J. You, Y. Sun et al., Studies on PEG-modified SLNs loading vinorelbine bitartrate (I): preparation and evaluation in vitro. Int. J. Pharm. **359**, 104–110 (2008)
35. K. Manjunath, V. Venkateswarlu, A. Hussain, Preparation and characterization of nitrendipine solid lipid nanoparticles. Pharmazie **66**, 178–186 (2011)
36. M. Üner, Preparation, characterization and physicochemical properties of solid lipid nanoparticles (SLN) and nanostructured lipid carriers (NLC): their benefits as colloidal drug carrier systems. Pharmazie **61**, 375–386 (2006)
37. H. Bunjes, M.H.J. Koch, K. Westesen, Influence of emulsifiers on the crystallization of solid lipid nanoparticles. J. Pharm. Sci. **92**, 1509–1520 (2003)
38. A. Lippacher, R.H. Müller, K. Mäder, Semisolid SLN^{TM} dispersions for topical application: influence of formulation and production parameters on viscoelastic properties. Eur. J. Pharm. Biopharm. **53**, 155–160 (2002)
39. A. Dingler, R.P. Blum, H. Niehus et al., Solid lipid nanoparticles (SLN^{TM}/Lipopearls^{TM}) – a pharmaceutical and cosmetic carrier for the application of vitamin E in dermal products. J. Microencapsul. **16**, 751–767 (1999)
40. W. Mehnert, K. Mäder, Solid lipid nanoparticles. Production, characterization and applications. Adv. Drug Deliv. Rev. **47**, 165–196 (2001)
41. V.B. Patravale, A.V. Ambarkhane, Study of solid lipid nanoparticles with respect to particle size distribution and drug loading. Pharmazie **58**, 392–395 (2003)
42. C. Freitas, R.H. Müller, Spray-drying of solid lipid nanoparticles (SLN^{TM}). Eur. J. Pharm. Biopharm. **46**, 145–151 (1998)
43. A. Califice, F. Michel, G. Dislaire et al., Influence of particle shape on size distribution measurements by 3D and 2D image analyses and laser diffraction. Powder Technol. **237**, 67–75 (2013)
44. R.H. Müller, W. Mehnert, *Particle and Surface Characterisation Methods* (Wissenschaftliche Verlagsgesellschaft, Stuttgart, 1997)
45. M. Üner, R.H. Müller, Sage extract entrapped in nanostructured lipid carriers for application into the mouth cavity for oral hygiene. Curr. Top. Nutraceutical Res. **10**, 193–200 (2012)
46. M. Üner, Solid lipid nanoparticles and nanostructured lipid carriers for cancer therapy, in *Handbook of Clinical Nanomedicine – From Bench to Bedside,* ed. by R. Bawa, G.F. Audette, I. Rubinstein (Raj Bawa, Series Editor). Pan Stanford Series in Nanomedicine, vol. 1 (Pan Stanford Publishing, Singapore, 2015 in press)
47. http://nanocomposix.com
48. C. Freitas, R.H. Müller, Effect of light and temperature on zeta potential and physical stability in solid lipid nanoparticle (SLN^{TM}) dispersions. Int. J. Pharm. **168**, 221–229 (1998)
49. R.H. Müller, *Zetapotential und Partikelladung-Kurze Theorie, praktische Mesdurchfuhrung, Dateninterpretation* (Wissenschaftliche Verlagsgesellschaft mbH, Stuttgart, 1996)

50. R. Cavalli, O. Caputo, M.E. Carlotti et al., Sterilization and freeze-drying of drug-free and drug-loaded solid lipid nanoparticles. Int. J. Pharm. **148**, 47–54 (1997)
51. M. Üner, G. Yener, Importance of solid lipid nanoparticles (SLN) in various administration routes and future perspectives. Int. J. Nanomed. **2**, 289–300 (2007)
52. X.-Y. Ying, D. Cui, L. Yu et al., Solid lipid nanoparticles modified with chitosan oligosaccharides for the controlled release of doxorubicin. Carbohydr. Polym. **84**, 1357–1364 (2011)
53. C. Carrillo, N. Sánchez-Hernández, E. García-Montoya et al., DNA delivery via cationic solid lipid nanoparticles (SLNs). Eur. J. Pharm. Sci. **49**, 157–165 (2013)
54. V. Klang, C. Valenta, N.B. Matsko, Electron microscopy of pharmaceutical systems. Micron **44**, 45–74 (2013)
55. R. Erni, M.D. Rossell, C. Kisielowski et al., Atomic-resolution imaging with a sub-50-pm electron probe. Phys. Rev. Lett. **102**, 96–101 (2009)
56. K. Jores, W. Mehnert, M. Drechsler et al., Investigations on the structure of solid lipid nanoparticles (SLN) and oil-loaded solid lipid nanoparticles by photon correlation spectroscopy, field-flow fractionation and transmission electron microscopy. J. Control. Release **95**, 217–227 (2004)
57. I. Lacatusu, N. Badea, A. Murariu et al., The encapsulation effect of UV molecular absorbers into biocompatible lipid nanoparticles. Nanoscale Res. Lett. **6**, 73 (2011)
58. A. Dubes, H. Parrot-Lopez, W. Abdelwahed et al., Scanning electron microscopy and atomic force microscopy imaging of solid lipid nanoparticles derived from amphiphilic cyclodextrins. Eur. J. Pharm. Biopharm. **55**, 279–282 (2003)
59. S. Vahabi, B.N. Salman, A. Javanmard, Atomic force microscopy application in biological research: a review study. Iran. J. Med. Sci. **38**, 76–83 (2013)
60. H. Chen, X. Chang, D. Du et al., Podophyllotoxin-loaded solid lipid nanoparticles for epidermal targeting. J. Control. Release **110**, 296–306 (2006)
61. C. Olbrich, U. Bakowsky, C.M. Lehr et al., Cationic solid-lipid nanoparticles can efficiently bind and transfect plasmid DNA. J. Control. Release **77**, 345–355 (2001)
62. P. Shahgaldian, L. Quattrocchi, J. Gualbert et al., AFM imaging of calixarene based solid lipid nanoparticles in gel matrices. Eur. J. Pharm. Biopharm. **55**, 107–113 (2003)
63. P. Shahgaldian, E. Da Silva, A.W. Coleman et al., *Para*-acyl-calix-arene based solid lipid nanoparticles (SLNs): a detailed study of preparation and stability parameters. Int. J. Pharm. **253**, 23–38 (2003)
64. H. Bunjes, M.H.J. Koch, K. Westesen, Crystallization tendency and polymorphic transitions in triglyceride nanoparticles. Int. J. Pharm. **129**, 159–173 (1996)
65. J.S. Negi, P. Chattopadhyay, A.K. Sharma et al., Development and evaluation of glyceryl behenate based solid lipid nanoparticles (SLNs) using hot self-nanoemulsification (SNE) technique. Arch. Pharm. Res. **37**, 361–370 (2014)
66. M. Üner, E.F. Karaman, Z. Aydoğmuş, Solid lipid nanoparticles and nanostructured lipid carriers of loratadine for topical application: physicochemical stability and drug penetration through rat skin. Trop. J. Pharm. Res. **13**, 653–660 (2014)
67. K. Westesen, B. Siekmann, M.H.J. Koch, Investigations on the physical state of lipid nanoparticles by synchrotron radiation X-ray diffraction. Int. J. Pharm. **93**, 189–199 (1993)
68. R.H. Müller, W. Mehnert, J.S. Lucks et al., Solid lipid nanoparticles (SLN) – an alternative colloidal carrier system for controlled drug delivery. Eur. J. Pharm. Biopharm. **41**, 62–69 (1995)
69. A. Zur Mühlen, C. Schwarz, W. Mehnert, Solid lipid nanoparticles (SLN) for controlled drug delivery-Drug release and release mechanism. Eur. J. Pharm. Biopharm. **45**, 149–155 (1998)
70. B. Siekmann, K. Westesen, Thermoanalysis of recrystallisation process of melt-homogenized glyceride nanoparticles. Colloids Surf. B: Biointerfaces **3**, 159–175 (1994)
71. V. Venkateswarlu, K. Manjunath, Preparation, characterization and in vitro release kinetics of clozapine solid lipid nanoparticles. J. Control. Release **95**, 627–638 (2004)
72. J.L. Ford, P. Timmins, *Pharmaceutical Thermal Analysis* (Ellis Horwood, Chichester, 1989)
73. C. Allais, G. Keller, P. Lesieur et al., X-ray diffraction/calorimetry coupling. A tool for polymorphism control. J. Therm. Anal. Calorim. **74**, 723–728 (2003)

74. A.I. Kitaigorodskii, *Organic Chemical Crystallography* (Springer, New York, 1984)
75. D.M. Small, *Handbook of Lipid Research*. The Physical Chemistry of Lipids (Plenum Press, New York, 1986)
76. C.W. How, R. Abdullah, R. Abbasalipourkabir, Physicochemical properties of nanostructured lipid carriers as colloidal carrier system stabilized with polysorbate 20 and polysorbate 80. Afr. J. Biotechnol. **10**, 1684–1689 (2011)
77. K. Jores, W. Mehnert, K. Mäder, Physicochemical investigations on solid lipid nanoparticles and on oil-loaded solid lipid nanoparticles: a nuclear magnetic resonance and electron spin resonance study. Pharm. Res. **20**, 1274–1283 (2003)
78. B. Angelov, A. Angelova, R. Mutafchieva et al., SAXS investigation of a cubic to a sponge (L_3) phase transition in self-assembled lipid nanocarriers. Phys. Chem. Chem. Phys. **13**, 3073–3081 (2011)
79. A. Illing, T. Unruh, M.H.J. Koch, Investigation on particle self-assembly in solid lipid-based colloidal drug carrier systems. Pharm. Res. **21**, 592–597 (2004)
80. C. Rümenapp, B. Gleich, A. Haase, Magnetic nanoparticles in magnetic resonance imaging and diagnostics. Pharm. Res. **29**, 1165–1179 (2012)
81. M.A. Schubert, M. Harms, C.C. Müller-Goymann, Structural investigations on lipid nanoparticles containing high amounts of lecithin. Eur. J. Pharm. Sci. **27**, 226–236 (2006)
82. E. Zimmermann, E.B. Souto, R.H. Müller, Physicochemical investigations on the structure of drug-free and drug-loaded solid lipid nanoparticles (SLN) by means of DSC and 1H NMR. Pharmazie **60**, 508–513 (2005)
83. M.S. Berkman, Y. Yazan, Solid lipid nanoparticles: a possible vehicle for zinc oxide and octocrylene. Pharmazie **67**, 202–208 (2012)
84. K. Jores, A. Haberland, S. Wartewig et al., Solid lipid nanoparticles (SLN) and oil-loaded SLN studied by spectrofluorometry and Raman spectroscopy. Pharm. Res. **22**, 1887–1897 (2005)
85. Y. Li, H.L. Wong, A.J. Shuhendler et al., Molecular interactions, internal structure and drug release kinetics of rationally developed polymer–lipid hybrid nanoparticles. J. Control. Release **128**, 60–70 (2008)